Polystyrene bound oxidovanadium(IV) and dioxidovanadium(V) complexes of histamine derived ligand for the oxidation of methyl phenyl sulfide, diphenyl sulfide and benzoin†

Mannar R. Maurya,*[a] Aarti Arya,[a] Amit Kumar[b] and João Costa Pessoa*[b]

Received 18th August 2008, Accepted 24th November 2008
First published as an Advance Article on the web 3rd February 2009
DOI: 10.1039/b814297a

Ligand Hsal–his (**I**) derived from salicylaldehyde and histamine has been covalently bound to chloromethylated polystyrene cross-linked with 5% divinylbenzene. Upon treatment with $[VO(acac)_2]$ in DMF, the polystyrene-bound ligand (abbreviated as PS–Hsal–his, **II**) gave the stable polystyrene-bound oxidovanadium(IV) complex PS–$[V^{IV}O$(sal–his)(acac)] **1**, which upon oxidation yielded the dioxidovanadium(V) PS–$[V^{V}O_2$(sal–his)] **2** complex. The corresponding non polymer-bound complexes $[V^{IV}O$(sal–his)(acac)] **3** and $[V^{V}O_2$(sal–his)] **4** have also been obtained. These complexes have been characterised by IR, electronic, ^{51}V NMR and EPR spectral studies, and thermal as well as scanning electron micrograph studies. Complexes **1** and **2** have been used as a catalyst for the oxidation of methyl phenyl sulfide, diphenyl sulfide and benzoin with 30% H_2O_2 as oxidant. Under the optimised reaction conditions, a maximum of 93.8% conversion of methyl phenyl sulfide with 63.7% selectivity towards methyl phenyl sulfoxide and 36.3% towards methyl phenyl sulfone has been achieved in 2 h with **2**. Under similar conditions, diphenyl sulfide gave 83.4% conversion where selectivity of reaction products varied in the order: diphenyl sulfoxide (71.8%) > diphenyl sulfone (28.2%). A maximum of 91.2% conversion of benzoin has been achieved within 6 h, and the selectivities of reaction products are: methylbenzoate (37.0%) > benzil (30.5%) > benzaldehyde-dimethylacetal (22.5%) > benzoic acid (8.1%). The PS-bound complex, **1** exhibits very comparable catalytic potential. These polymer-anchored heterogeneous catalysts do not leach during catalytic action, are recyclable and show higher catalytic activity and turnover frequency than the corresponding non polymer-bound complexes. EPR and ^{51}V NMR spectroscopy was used to characterise methanolic solutions of **3** and **4** and to identify species formed upon addition of H_2O_2 and/or acid and/or methyl phenyl sulfide.

Introduction

The coordination chemistry of vanadium has received increasing attention from researchers, particularly after the discovery of vanadate-dependent enzymes, vanadium haloperoxidases[1–3] from various sea algae and terrestrial fungi.[4] They are very active for the oxidative halogenation and oxidation of organic substrates in the presence of H_2O_2.[5,6] Various structural and functional models have been developed to understand the role of the enzyme and the mechanism of the reaction.[7] Generally, these functional models are homogeneous in nature and decompose during the catalytic reaction and thus are not suitable for industrial applications. Encapsulation of monomeric complexes in microporous materials such as zeolites[8] and mesoporous materials *e.g.* MCM-41,[9–12] or their immobilization onto polymer supports through covalent attachment are means to overcome this problem. Heterogenisation of homogeneous catalysts through their encapsulation or immobilization has the advantage of easy separation from the reaction mixture, leading to operational flexibility and their facile regeneration compared to homogeneous catalysts. Recently we have used chloromethylated polystyrene cross-linked with divinylbenzene, one of the most widely employed macromolecular supports,[13–16] for immobilization of model vanadium complexes and have tested their catalytic potential for a variety of oxidation reactions.[17–19]

Herein we report the preparation and characterisation of chloromethylated polystyrene-bound oxidovanadium(IV) and dioxidovanadium(V) complexes of Hsal–his (**I**), Scheme 1. The corresponding non polymer-bound complexes of **I**, which are considered as structural models of haloperoxidases, have also been prepared. Spectral evidence is presented for peroxide binding, in the presence of H_2O_2, to the vanadium centre. Catalytic potential

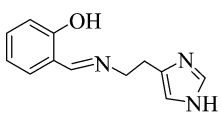

I: Hsal-his

Scheme 1

[a]*Department of Chemistry, Indian Institute of Technology Roorkee, Roorkee, 247 667, India. E-mail: rkmanfcy@iitr.ernet.in*
[b]*Centro Química Estrutural, Instituto Superior Técnico, TU Lisbon, Av Rovisco Pais, 1049-001, Lisboa, Portugal. E-mail: joao.pessoa@mail.ist.utl.pt*

† Electronic supplementary information (ESI) available: Electronic spectra, spin Hamiltonian parameters and ^{51}V NMR chemical shifts. See DOI: 10.1039/b814297a

of these complexes has been demonstrated by studying the oxidation of methyl phenyl sulfide, diphenyl sulfide and benzoin.

Experimental

Materials and methods

Chloromethylated polystyrene [18.9% Cl (5.3 mmol Cl per gram of resin)] cross-linked with 5% divinylbenzene was obtained as a gift from Thermax Limited, Pune, India. Analytical reagent grade V_2O_5 (Loba Chemie, India), 30% H_2O_2, salicylaldehyde (Ranbaxy, India), histamine hydrochloride, methyl phenyl sulfide, diphenyl sulfide (Himedia, India, or Acros, UK), benzoin (SRL, India) and other chemicals were used as purchased. $[VO(acac)_2]$[20] and Hsal–his[21] were prepared according to the methods reported in the literature.

Elemental analyses of the ligands and complexes were obtained by an Elementar model Vario-EL-III. IR spectra were recorded as KBr pellets on a Nicolet NEXUS Aligent 1100 FT-IR spectrometer. Electronic spectra of the polymer-bound complexes were recorded in Nujol on a Shimadzu 1601 UV-Vis spectrophotometer by layering a mull of the sample on the inside of one of the cuvettes while keeping the other one layered with Nujol as reference. Spectra of non polymer-bound ligand and complexes were recorded in methanol. The EPR spectra were recorded with a Bruker ESP 300E X-band spectrometer. For the polymer-anchored complex samples the spectra were measured at room temperature and also at 77 K after swelling in DMF; for the neat complexes the samples were frozen in either MeOH or DMF in liquid nitrogen and the EPR spectra were measured at 77 K. The spin Hamiltonian parameters were obtained by simulation of the spectra with the computer program of Rockenbauer and Korecz.[22] The ^{51}V NMR spectra were recorded on a Bruker Avance II+ 400 MHz (ultrashield magnet) instrument. Thermogravimetric analyses of the complexes were carried out using Perkin Elmer's PYRIS Diamond under oxygen atmosphere. The energy-dispersive X-ray analyses (EDX) of anchored ligand and complexes were recorded on a FEI Quanta 200 FEG. The samples were coated with a thin film of gold to prevent surface charging, to protect the surface material from thermal damage by the electron beam and to make the sample conductive. The identity of the products was confirmed using a GC-MS Perkin Elmer Clarus 500 and comparing the fragments of each product with the library available. A Thermax Nicolet gas chromatograph with a HP-1 capillary column (30 m × 0.25 μm × 0.25 μm) was used to analyse the reaction products and their quantifications were made on the basis of the relative peak area of the respective product.

Preparation of polymer-bound ligand, PS–Hsal–his II

Chloromethylated polystyrene (3.0 g) was allowed to swell in DMF (40 mL) for 2 h. A solution of Hsal–his (4.60 g, 25 mmol) in DMF (30 mL) was added to the above suspension followed by triethylamine (4.50 g) in ethylacetate (40 mL). The reaction mixture was heated at 90 °C for 15 h with slow mechanical stirring. After cooling to room temperature, the yellow resins were separated by filtration, washed thoroughly with hot DMF followed by hot methanol and dried in an air oven at 120 °C. (Found: C, 74.40; H, 11.61; N, 9.41%).

Preparation of complexes

PS–[V^{IV}O(sal–his)(acac)] 1. Polymer-anchored ligand PS–Hsal–his (2.00 g) was allowed to swell in DMF (25 mL) for 2 h. A solution of $[VO(acac)_2]$ (5.30 g, 20 mmol) in 20 mL DMF was added to the above suspension and the reaction mixture was heated at 90 °C for 14 h with slow mechanical stirring. After cooling to room temperature, the dark black polymer-anchored complex was separated by filtration, washed with hot DMF followed by hot methanol and dried at 120 °C in an air oven. (Found: C, 68.56; H, 10.24; N, 7.45; V, 8.89%).

PS–[$V^{V}O_2$(sal–his)] 2.

Method A. A solution of KVO_3 was generated *in situ* by dissolving V_2O_5 (5.46 g, 30 mmol) in aqueous KOH (3.36 g, 60 mmol in 50 mL H_2O). PS–Hsal–his (2 g) was suspended in the above solution and stirred mechanically for *ca.* 48 h at which point the colour of the beads had changed to orange. They were separated by filtration, washed with water followed by methanol and dried in a desiccator. (Found: C, 67.13; H, 9.12; N, 6.96; V, 8.41%).

Method B. Complex, PS–[V^{IV}O(sal–his)(acac)] **1** (1.5 g) was suspended in methanol (40 mL) and air was bubbled through the suspension for *ca.* 4 d. During this period the colour of the beads slowly changed to orange. They were separated by filtration, washed with water followed by methanol and dried in a desiccator. (Found: C, 67.10; H, 9.14; N, 6.94; V, 8.43%).

[V^{IV}O(sal–his)(acac)] 3. Complex **3** was prepared according to the reported procedure.[21] Yield 65%. (Found: C, 53.21; H, 5.54; N, 10.85; V, 12.83%. Calcd for $C_{18}H_{23}N_3O_5V$: C, 53.27; H, 5.78; N, 10.96; V, 13.29%).

[$V^{V}O_2$(sal–his)] 4. Complex **3** (0.383 g, 1 mmol) was dissolved in 50 mL of methanol and after addition of aqueous 30% H_2O_2 (0.2 mL) air was gently passed through the solution for 4 d. During this period the V^{IV} in **3** completely oxidized and the solution became yellow. The yellow solid of **4** was obtained after reducing the solvent volume to *ca.* 5 mL, which was filtered and dried *in vacuo*. Yield 63%. (Found: C, 48.24; H, 3.96; N, 13.93; V, 16.42%. Calcd for $C_{12}H_{12}N_3O_3V$: C, 48.50; H, 4.07; N, 14.14; V, 17.14%.) ^1H NMR (DMSO-d_6, δ/ppm): 12.82 (s, 1H,–NH), 8.70 (s, 1H,–CH=N–), 8.07 (s, 1H), 7.47 (s, 1H), 7.37 (s, 1H), 7.12 (s, 1H), 6.74 (s, 1H), 6.72 (d, 1H) (aromatic), 3.91 (b, 4H,–CH_2). ^{51}V NMR (MeOD-d_4, δ/ppm): −547).

Catalytic activity studies

Oxidation of methyl phenyl sulfide, diphenyl sulfide and benzoin was carried out in 50 mL reaction flasks.

Oxidation of methyl phenyl sulfide and diphenyl sulfide. The polymer-anchored catalyst, after swelling in methanol for 2 h, was used for the oxidation of methyl phenyl sulfide and diphenyl sulfide. Methyl phenyl sulfide (1.24 g, 10 mmol) or diphenyl sulfide (1.86 g, 10 mmol), 30% aqueous H_2O_2 (1.71 g, 15 mmol), and catalyst (0.045 g) in 10 mL acetonitrile were stirred at room temperature and the reaction was monitored by withdrawing samples at different time intervals and analysing them quantitatively by gas chromatography. The identities of the products were confirmed by GC-MS. Various parameters such as the amount of oxidant

and catalyst were considered in order to study their effect on the reaction products.

Oxidation of benzoin. In a typical oxidation reaction, benzoin (1.06 g, 5 mmol), aqueous 30% H_2O_2 (1.71 g, 15 mmol) and catalyst (0.030 g) were mixed in 25 mL methanol. The reaction mixture was heated under reflux with stirring for 6 h. The progress of the reaction was monitored as mentioned above. The effect of various parameters such as temperature, amount of oxidant and catalyst were checked to optimise the conditions for the best performance of the catalyst.

Results and discussion

Synthesis, reactivity and solid state characteristics

Reaction of Hsal–his with chloromethylated polystyrene, cross-linked with 5% divinylbenzene in DMF in the presence of triethylamine gave the polymer-anchored ligand, PS–Hsal–his. The reaction was carried out at 90 °C. At this temperature the ligand did not decompose. Miller and Sherrington have used refluxing toluene to carry out the anchoring of 2-(2-pyridyl)imidazole through covalent attachment of the imine nitrogen to chloromethylated polystyrene.[23] During this process the –NH group of histamine reacts with the $–CH_2Cl$ group as shown in Scheme 2. The remaining chlorine content of 1.5% (0.42 mmol Cl per gram of resin) in the PS-bound ligand suggests ~92% loading of the ligand.

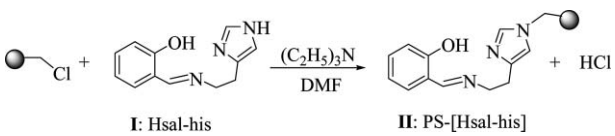

I: Hsal-his **II**: PS-[Hsal-his]

Scheme 2 Reaction of Hsal–his with chloromethylated polystyrene.

The anchored ligand on reaction with $[V^{IV}O(acac)_2]$ in DMF resulted in the formation of the oxidovanadium(IV) complex PS–$[V^{IV}O$(sal–his)(acac)] **1**. The chloromethylated group does not coordinate with the vanadium precursor. Aerobic oxidation of **1** in methanol is very slow but gave the dioxidovanadium(V) complex PS–$[V^{V}O_2$(sal–his)] (**2**). Eqns 1 and 2 summarise the synthetic procedures.

$$\text{PS–Hsal–his} + [V^{IV}O(acac)_2] \rightarrow \text{PS–}[V^{IV}O\text{(sal–his)(acac)}] + \text{Hacac} \quad (1)$$

$$2\ \text{PS–}[V^{IV}O\text{(sal–his)(acac)}] + \tfrac{1}{2}O_2 + H_2O \rightarrow 2\ \text{PS–}[V^{V}O_2\text{(sal–his)}] + 2\text{Hacac} \quad (2)$$

Table 1 provides data of metal and ligand loading in polymer-anchored complexes assuming the formation of PS–Hsal–his. The data show that the metal to ligand ratio in polymer-bound complexes is close to 1 : 1.

The structure of non polymer-bound oxidovanadium(IV) complex **3** (refer to Scheme 5) has already been established by an X-ray single crystal study by Pecoraro and co-workers.[21] Aerobic oxidation of **3** in the presence of a few drops of aqueous 30% H_2O_2 results in the formation of dioxidovanadium(V) complex **4**, which is now characterised by elemental and spectroscopic (IR, UV-vis, ^1H and ^{51}V NMR) studies. The corresponding polymer-bound complex **2** is proposed to have a similar binding mode.

Table 1 Ligand and metal loadings in polymer-bound complexes, and ligand-to-metal ratio data

Compound	Ligand loading (mmol g^{-1} of resin)	Metal ion loading[a] (mmol g^{-1} of resin)	Ligand : Metal ratio
PS–[Hsal–his] **I**	2.24	—	—
PS–$[V^{IV}O$(sal–his)(acac)] **1**	1.66	1.74	1:0.95
PS–$[V^{V}O_2$(sal–his)] **2**	1.77	1.65	1:1.07

[a] $\text{Metal ion loading} = \dfrac{\text{Observed metal\%} \times 100}{\text{Atomic mass of metal}}$.

Field emission scanning electron microscope (FE-SEM) and energy-dispersive X-ray analysis (EDX) studies

Field emission scanning electron micrographs (FE-SEM) and energy-dispersive X-ray analysis (EDX) profiles for a single bead of polymer-bound ligand and the vanadium complexes were recorded to observe the morphological changes. Some of these images along with the energy-dispersive X-ray analysis (EDX) profile are reproduced in Fig. 1. As expected, the pure polystyrene bead has a smooth and flat surface while the polymer-bound ligand and complexes show a very slight roughening of the top layer. This roughening is more noticeable in complexes **1** and **2** possibly due to the interaction of vanadium with the polymer-bound ligand which results in the formation of a complex with a fixed geometry. Accurate information on the morphological changes in terms of exact orientation of ligands coordinated to the metal ion has not been possible due to poor loading of the metal complex. However, pure polymer beads show mainly two components on the surface—carbon (80.7%) and chlorine (18.3%)—as evaluated semi-quantitatively by energy-dispersive X-ray analysis. A considerable amount of N (*ca.* 8.1%) and a

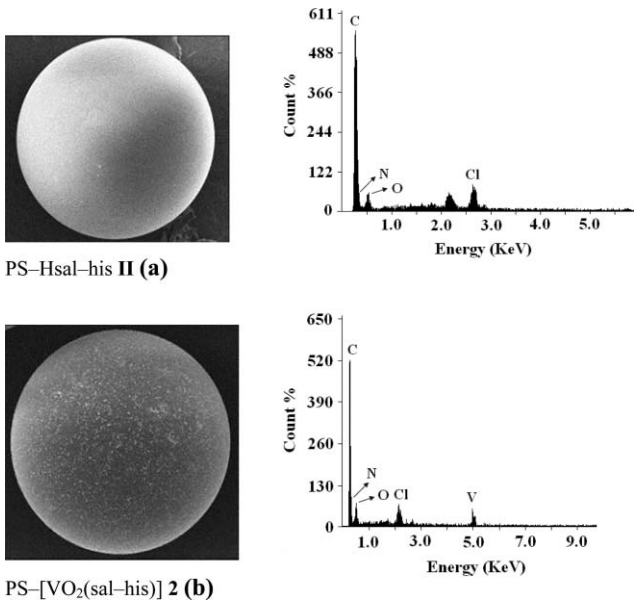

PS–Hsal–his **II** **(a)**

PS–$[VO_2$(sal–his)] **2** **(b)**

Fig. 1 FE-SEM (left) and energy-dispersive X-ray analysis (EDX) profile (right) of (a) PS–Hsal–his **II** and (b) PS–$[V^{V}O_2$(sal–his)] **2**.

small amount of Cl (*ca.* 2.1%), were determined on the surface of the beads containing bound ligand. The polystyrene beads of immobilized metal complexes PS–[$V^{IV}O$(sal–his)(acac)] and PS–[$V^{V}O_2$(sal–his)] also contain significant amounts of metal along with nitrogen, suggesting the formation of a metal complex with the anchored ligand at various sites.

TGA study

Thermogravimetric analysis under an oxygen atmosphere shows the good stability of polymer-anchored complexes **1** and **2** up to *ca.* 200 °C and thereafter they decompose exothermically in several steps. Quantitative measurement of weight loss at various stages was not possible due to their overlapping nature. However, the residues due to the metal oxides obtained as the end product at *ca.* 850 °C (in **1**) and at *ca.* 500 °C (in **2**) indicate that the metal complexes are covalently bound to the polymer. The decomposition of **1** is completed in four steps. Two overlapping steps occur in the temperature range 200–395 °C. At this stage the decomposed product is quite stable. The next weight loss starts at 725 °C and continues until the formation of end product. The observed residue of 29.8% is close to the calculated value of 29.2% for V_2O_5 at 850 °C. The first weight loss step in non polymer-bound complex **2** starts at *ca.* 200 °C and is completed at 290 °C with a weight loss of 42%. The second weight loss step amounting to 7.6% starts at *ca.* 290 °C and is completed at 375 °C. The final step starts at 375 °C and is completed at *ca.* 450 °C with a total weight loss of 68.7%. The final residue of 31.3% (calcd 30.6%) suggests the formation of V_2O_5 as the end product.

IR spectral study

A partial list of IR spectral data of the polymer-anchored ligand and complexes along with non-polymer bound ones are listed in Table 2. The Hsal–his (**I**) ligand exhibits a sharp band at 1632 cm^{-1} due to ν(C=N) (azomethine), and this band shifts to lower wavenumbers by 32 cm^{-1} (in **3**) and 21 cm^{-1} in **4** suggesting the coordination of azomethine nitrogen to the metal ion. The polymer-anchored ligand PS–Hsal–his (**II**) exhibits a sharp band at 1639 cm^{-1} due to the ν(C=N) stretch, and in the polymer-anchored complexes this band shows up at 1612–1617 cm^{-1}. This observation suggests the coordination of the azomethine nitrogen atom to the metal ion. The additional band observed at *ca.* 1630 cm^{-1} in all complexes is possibly due to coordination of the imidazole nitrogen atom.

The polymer-bound complex **1** exhibits a sharp band at 986 cm^{-1} due to ν(V=O) while **2** exhibits two such bands at 960 and 931 cm^{-1} corresponding to ν_{asym}(O=V=O) and ν_{sym}(O=V=O) modes, respectively.[21] As shown in Table 2, the corresponding non polymer-bound vanadium complexes display these bands at

Table 2 IR spectral data

Compound	(C=N)	(V=O)
Hsal–his **I**	1632	—
[VO(acac)(sal–his)] **3**	1600	945
[VO_2(sal–his)] **4**	1611	927, 895
PS-Hsal–his **II**	1639	—
PS–[VO(acac)(sal–his)] **1**	1612	986
PS–[VO_2(sal–his)] **2**	1617	960, 931

Table 3 Spin Hamiltonian parameters

Complex	Solvent	$g_{\parallel}$	$A_{\parallel}$ ($\times 10^4$ cm^{-1})	$g_{\perp}$	$A_{\perp}$ ($\times 10^4$ cm^{-1})
PS–[$V^{IV}O$ (sal–his)(acac)] **1**	Solid	1.949	163.8	1.980	58.6
	DMF	1.952	164.8	1.980	57.5
[$V^{IV}O$(sal–his) (acac)] **3**	MeOH	1.953	161.5	1.981	56.0
	DMF	1.954	161.5	1.980	55.7

945 cm^{-1} (in **3**), and at 927 and 895 cm^{-1} (in **4**) similar to other examples reported in the literature.[24]

Electronic spectral study

Electronic spectra (Fig. S1 and S2) and spectral data (Table S1) of ligands and complexes are given in the ESI†.

EPR Spectroscopy study

The 1st derivative EPR spectra have been recorded for "frozen" MeOH and DMF solutions of complex **3** and for **1** in the solid state at room temperature. The EPR spectra of **1** and **3** are shown in Fig. 2. The spectrum of **1** is characteristic of magnetically diluted $V^{IV}O$-complex and the well-resolved EPR hyperfine features indicate that the vanadium(IV) centers are well dispersed in the polymer matrix. Comparison with the spectra of **3** in MeOH and DMF indicates that the coordination environments of **1** and **3** are the same and as reported by Cornman *et al.*[21] The value of $A_{\parallel}$ can be estimated using the additivity relationship proposed by Wuethrich[25] and Chasteen,[26a] with estimated accuracy of $\pm 3 \times 10^{-4}$ cm^{-1}, and we do not expect any significant influence from the axial ligand.[26b] The spectra were simulated and the spin Hamiltonian parameters obtained[22] are included in Table 3. By using the following partial contributions (O_{acac}, 37.6; $O_{phenolate}$, 38.9; N_{imine}, 41.6; N_{imid}, 45×10^{-4} cm^{-1})$_{equatorial}$(O_{acac})$_{axial}$,[27] an estimated $A\|$ of 163.1 $\times 10^{-4}$ cm^{-1} is obtained. We can therefore conclude that the spectra are consistent with such a binding mode. The contribution of imidazole (N_{imid}) may depend on its orientation with respect to the V=O bond, ranging from 40 (parallel, best orbital overlap) to 45×10^{-4} (perpendicular).[27] For the N_{imid} of the sal–his ligand, taking into account the known molecular structure in the solid state,[21] we expect the imidazole ring to be positioned perpendicular to the V=O group, so that a contribution close to 45×10^{-4} is predicted.

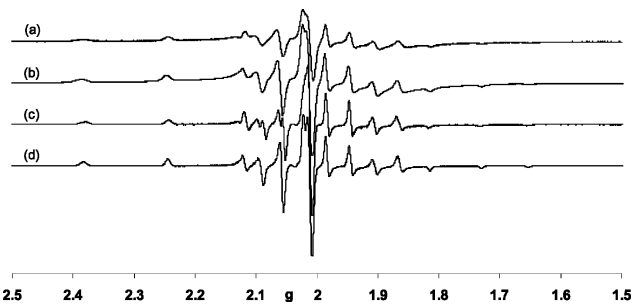

Fig. 2 1st derivative EPR spectra of PS–[$V^{IV}O$(sal–his)(acac)] **1**: (a) solid at room temperature, (b) in contact with DMF at 77K; and [VO^{IV}(sal–his)(acac)] **3**: (c) in MeOH at 77K, (d) in DMF at 77K.

Catalytic activity studies

The catalytic potential of the polymer-bound complexes **1** and **2** as well as their non polymer-bound analogues were explored for the oxidation of methyl phenyl sulfide, diphenyl sulfide and benzoin.

Oxidation of methyl phenyl sulfide and diphenyl sulfide. The oxidation of sulfides is catalysed by a variety of vanadyl,[28] manganese[29] and titanium complexes.[30] Methyl phenyl sulfide and diphenyl sulfide have electron-rich sulfur atoms which, on electrophilic oxidation, give sulfoxide and, upon further oxidation, sulfone (see Scheme 3).

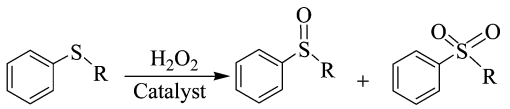

R = CH_3: Methyl phenyl sulfide
R = C_6H_5: Diphenyl sulfide

Scheme 3 Oxidation of organic sulfides.

Complexes PS–[$V^{IV}O$(sal–his)(acac)] **1** and PS–[$V^{V}O_2$(sal–his)] **2** have been used as catalysts for the oxidation of these sulfides by using aqueous 30% H_2O_2. Reaction conditions have been optimised for the maximum oxidation of methyl phenyl sulfide and diphenyl sulfide considering **2** as a representative catalyst while varying the amount of oxidant and catalyst.

The effect of the H_2O_2 concentration on the oxidation of methyl phenyl sulfide is illustrated in Fig. 3(a). Using three different concentrations of aqueous 30% H_2O_2, *viz*. 10 mmol (1.14 g), 15 mmol (1.71 g) and 20 mmol (2.27 g) with fixed amounts of methyl phenyl sulfide (1.24 g, 10 mmol) and PS–[$V^{V}O_2$(sal–his)] (0.025 g) in CH_3CN (15 mL), the conversions of methyl phenyl sulfide obtained were 63.8, 93.8 and 96.3%, respectively, in 2 h at room temperature. No appreciable improvement in the conversion is noted on increasing the oxidant to substrate molar ratios. Thus, the oxidant to substrate ratio of 1.5 : 1 may be considered as the most suitable at the expense of oxidant for the maximum oxidation of methyl phenyl sulfide.

For three different amounts *viz*. 0.015, 0.025 and 0.035 g of catalyst and methyl phenyl sulfide to H_2O_2 molar ratio of 1 : 1.5 under the reaction conditions given above, 0.015 g of catalyst gave only 75.0% conversion. Increasing this amount to 0.025 g gave a conversion of 93.8% while 0.035 g of catalyst has shown only slight improvement in the conversion (Fig. 3(b)). Thus, 0.025 g of catalyst was considered adequate to run the reaction under these conditions.

Thus, the optimised reaction conditions obtained for the maximum oxidation of 10 mmol of methyl phenyl sulfide are: catalyst (0.025 g), H_2O_2 (1.71 g, 15 mmol), and CH_3CN (15 mL). At least 2 h are required to complete the reaction. Similarly for 10 mmol of diphenyl sulfide, 0.045 g of catalyst and H_2O_2 : diphenyl sulfide molar ratio of 3 : 1 in 15 mL of acetonitrile was found to be the best to give a maximum of 83.4% conversion of diphenyl sulfide in 3 h of reaction time at room temperature. Catalyst, PS–[$V^{IV}O$(sal–his)(acac)] **1**, under the above reaction conditions gave lower conversion (Table 4) for methyl phenyl sulfide as well as for diphenyl sulfide. Selectivity details for the products obtained for the oxidation of methyl phenyl sulfide and diphenyl sulfide are presented in Table 4. It is clear from the table that catalyst PS–[$V^{V}O_2$(sal–his)]

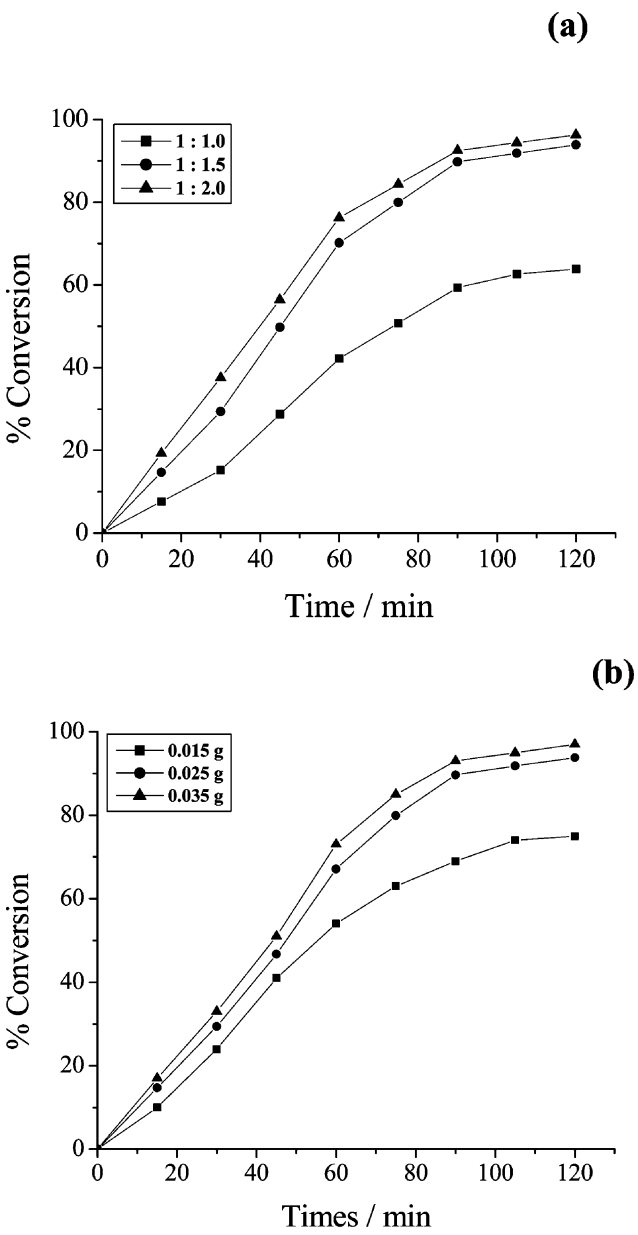

Fig. 3 **(a)** Effect of amount of H_2O_2 on the oxidation of methyl phenyl sulfide. Reaction conditions: methyl phenyl sulfide (1.24 g, 10 mmol), PS–[$V^{V}O_2$(sal–his)] (0.025 g) in CH_3CN (15 mL). **(b)** Effect of amount of catalyst PS–[$V^{V}O_2$(sal–his)] on the oxidation of methyl phenyl sulfide. Reaction conditions: methyl phenyl sulfide (1.24 g, 10 mmol), H_2O_2 (1.71 g, 15 mmol) in CH_3CN (15 mL).

has good catalytic potential for both substrates with high turn over frequency. But the selectivity for the formation of methyl phenyl sulfoxide is better (71.8%) than for diphenyl sulfoxide (63.7%).

The catalytic activity of non polymer-bound complexes [$V^{V}O_2$(sal–his)] **4** and [$V^{IV}O$(sal–his)(acac)] **3** using the same mole concentration as used for the polymer-anchored complexes under reaction conditions established above has also been tested for comparison. Comparative profiles for the conversion of methyl phenyl sulfide and diphenyl sulfide using neat as well as polymer-bound complexes are also presented in Table 4. Conversions of both sulfides using neat complex are also very good, but always lower than their polymer-bound analogues. The selectivity for sulfoxide

Table 4 Conversion of sulfides, TOF and product selectivity data

Substrate	Catalyst	Conv. (%)	TOF[a] (h^{-1})	% Selectivity	
				Sulfoxide	Sulfone
Methyl phenyl sulfide	PS–[$V^{V}O_2$(sal–his) **2**	93.8	113.8	63.7	36.3
	[$V^{V}O_2$(sal–his)] **4**	84.8	96.4	61.0	39.0
	PS–[$V^{IV}O$(sal–his)(acac)] **1**	79.5	91.2	64.8	35.2
	[$V^{IV}O$(sal–his)(acac)] **3**	72.1	83.3	62.9	37.1
Diphenyl sulfide	PS–[$V^{V}O_2$(sal–his)] **2**	83.4	37.5	71.8	28.2
	[$V^{V}O_2$(sal–his)] **4**	70.7	30.2	67.8	32.2
	PS–[$V^{IV}O$(sal–his)(acac)] **1**	67.4	28.7	73.1	26.9
	[$V^{IV}O$(sal–his)(acac)] **3**	60.3	19.8	68.9	31.1

[a] TOF values in moles of product per mole of catalyst.

formation is also lower with neat complex (Table 4). Blank reactions using methyl phenyl sulfide (1.24 g, 10 mmol), aqueous 30% H_2O_2 (1.71 g, 15 mmol) and acetonitrile (15 mL) resulted in 15.2% conversion with selectivity sulfoxide : sulfone of 68 : 32. Blank reactions for diphenyl sulfide under the reaction conditions above gave only 5.5% conversion with sulfoxide : sulfone selectivity of 57 : 43.

Oxidation of benzoin. The selective oxidation of α-hydroxyketones to α-diketones is one of the important reactions in fine chemical synthesis.[31–35] The oxidation of benzoin has attracted the attention of researchers because one of its oxidised products, benzil, is a very useful intermediate for the synthesis of heterocyclic compounds and benzylic acid rearrangements.[36] Here, the oxidation of benzoin was successfully achieved with the catalyst PS–[$V^{V}O_2$(sal–his)] **2** using 30% aqueous H_2O_2 as oxidant. Before starting the catalytic run, the catalyst was allowed to swell in methanol for 2 h so that the active sites of the catalyst in the polymer cavity are easily accessible to the substrate and oxidant. The products mainly obtained were benzil, methylbenzoate, benzoic acid and benzaldehyde-dimethylacetal (Scheme 4).

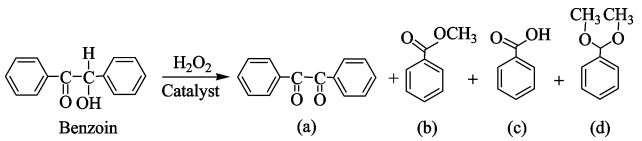

Scheme 4 Oxidized products of benzoin: (a) benzil, (b) methyl benzoate, (c) benzoic acid and (d) benzaldehyde-dimethylacetal.

To optimise the reaction conditions for the maximum oxidation of benzoin, the effect of oxidant was studied by considering oxidant to substrate ratios of 2 : 1, 3 : 1 and 4 : 1 for the fixed amount of catalyst (0.030 g) and substrate (1.06 g, 5 mmol) in 25 mL of refluxing methanol. At the oxidant to substrate ratio of 3 : 1, maximum conversion of benzoin was achieved in 6 h of reaction time.

Similarly, among four different amounts of catalysts *e.g.* 0.015, 0.030, 0.050 and 0.070 g for the fixed amount of benzoin (1.06 g, 5 mmol) and 30% H_2O_2 (1.7 g, 15 mmol) in 25 mL of methanol at the reflux temperature, the oxidation of benzoin was slow for the first 1.5 h with 0.015 g of catalyst, then reached 71.8% in *ca.* 6 h. Increasing the catalyst amount to 0.030 g resulted in significant improvement; here the conversion reached 91.2% within 6 h of reaction time, followed by no further improvement with time. Further increasing the amount of catalyst to 0.050 or 0.070 g did not show considerable improvement either in the oxidation of benzoin or in the reduction in time to reach the steady-state in the reaction processes.

Fig. 4 presents the selectivity of products along with the conversion of benzoin as a function of time (6 h) under the optimal experimental conditions as concluded above, *i.e.* benzoin (1.10 g, 5 mmol), 30% H_2O_2 (1.7 g, 15 mmol), PS–[$V^{V}O_2$(sal–his)] (0.030 g, 0.014 mmol) and methanol (25 mL). It is clear from the plot that all products (four identified and one unidentified) form from the conversion of benzoin. With the highest selectivity of benzil (*ca.* 50%) at the beginning, a continuous but slow decrease with time of its selectivity has been observed which finally reaches 30.5% after 6 h. The selectivity of benzoic acid and benzaldehyde-dimethylacetal only marginally increases while that of methyl benzoate increases considerably from 15 to 37%. Thus, with the maximum benzoin oxidation of 91.2% after 6 h of reaction time, the selectivities of the reaction products vary in the order: methyl benzoate (37%) > benzil (30.5%) > benzaldehyde-dimethylacetal (22.5%) > benzoic acid (8.1%). These data are summarised in Table 5.

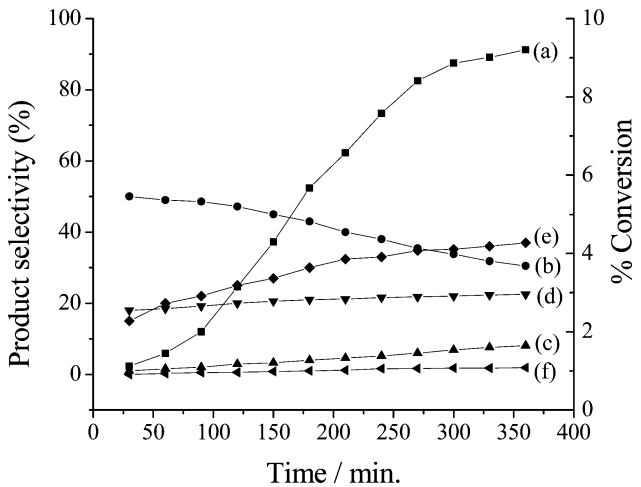

Fig. 4 Time *vs.* product selectivity distribution plot for the conversion of benzoin (a) using PS–[$V^{V}O_2$(sal–his)] as a catalyst, (b) benzil, (c) benzoic acid, (d) benzaldehyde-dimethylacetal, (e) methyl benzoate and (f) others (not identified).

The catalytic activity of PS–[$V^{IV}O$(sal–his)(acac)] **1** is not so good giving 83.4% conversion of benzoin, the selectivity of the different products being nearly the same. The performance of neat complexes using the same mole concentrations as used for

Table 5 Percent conversion of benzoin and selectivities of various oxidation products

Catalyst	Conv. (%)	Product selectivity (%)[a]					TOF/h^{-1}
		a	b	c	d	Others	
PS–[$V^{V}O_2$(sal–his)] **2**	91.2	30.5	8.1	22.5	37.0	1.9	15.4
[$V^{V}O_2$(sal–his)] **4**	76.4	27.8	13.2	19.6	36.8	2.6	12.2
PS–[$V^{IV}O$(sal–his)(acac)] **1**	83.4	31.2	5.8	23.4	37.5	2.1	14.1
[$V^{IV}O$(sal–his)(acac)] **3**	70.7	29.5	12.2	20.2	35.2	2.3	11.3

[a] For details of abbreviations see Scheme 4.

polymer-anchored complexes has also been studied under the optimised conditions. Thus, 0.0048 g (0.016 mmol) of catalyst [$V^{V}O_2$(sal–his)] **4** was added to a mixture of benzoin (1.10 g, 5 mmol) and 30% H_2O_2 (1.7 g, 15 mmol) in 25 mL of methanol, and the reaction products were analysed as a function of time. It was observed that the neat catalyst is also very active and gave 76.4% conversion in 6 h of reaction time. Here, selectivity of the various products varies in the order: methylbenzoate (36.8%) > benzil (27.8%) > benzaldehyde-dimethylacetal (19.6%) > benzoic acid (13.2%) *i.e.* the same order as obtained for the polymer-bound catalyst. A maximum of 70.7% conversion has been obtained with [$V^{IV}O$(sal–his)(acac)] **3** with similar selectivity under the conditions above. The turnover frequencies for the polymer-anchored complexes are 14.1 (for **1**) and 15.4 (for **2**) and are higher than those obtained for the non polymer-bound complexes. Moreover, the easy removal of the polymer-bound catalysts makes them better compared with their non polymer-bound counterparts.

Reactivity of non-polymer bound complexes with H_2O_2

Solutions of [$V^{IV}O$(sal–his)(acac)] **3** in methanol are sensitive towards addition of H_2O_2, as monitored by electronic absorption spectroscopy, yielding oxoperoxo species. Fig. 5 presents the spectral changes observed for **3**. Thus, the progressive addition of a dilute H_2O_2 solution in methanol to a solution of [$V^{IV}O$(sal–his)(acac)] **3** in methanol results first in flattening of the band appearing at 776 nm; upon further addition of one drop portions of the H_2O_2 solution this band disappears. The intensity of the 532 nm band slowly increases, while the band at 382 nm gradually shifts to 394 nm. At the same time new bands appear at 319 and 257 nm, while the intensity of the 265 nm band also increases. These changes indicate the interaction of [$V^{IV}O$(sal–his)(acac)] with H_2O_2 in methanol. The disappearance of *d*–*d* bands is in accordance with the oxidation of the $V^{IV}O$ complex to an oxidoperoxovanadium(v), and the band appearing at *ca*. 425 nm is probably due to a LMCT band of the monoperoxo complex.

The spectral changes during a similar titration of **4** with H_2O_2 in methanol is shown in Fig. S3 of the ESI†. With low amounts of H_2O_2 added no appreciable changes in band positions were observed, but further additions of H_2O_2 yielded a final spectrum which is very similar to that obtained in the titration of [$V^{IV}O$(sal–his)(acac)] **3** with H_2O_2, thus demonstrating that the same oxidoperoxovanadium(v) species form upon addition of H_2O_2 to methanolic solutions of either **3** or **4**. Upon further additions of H_2O_2 (2 mmol of 30% H_2O_2 dissolved in 5 mL of

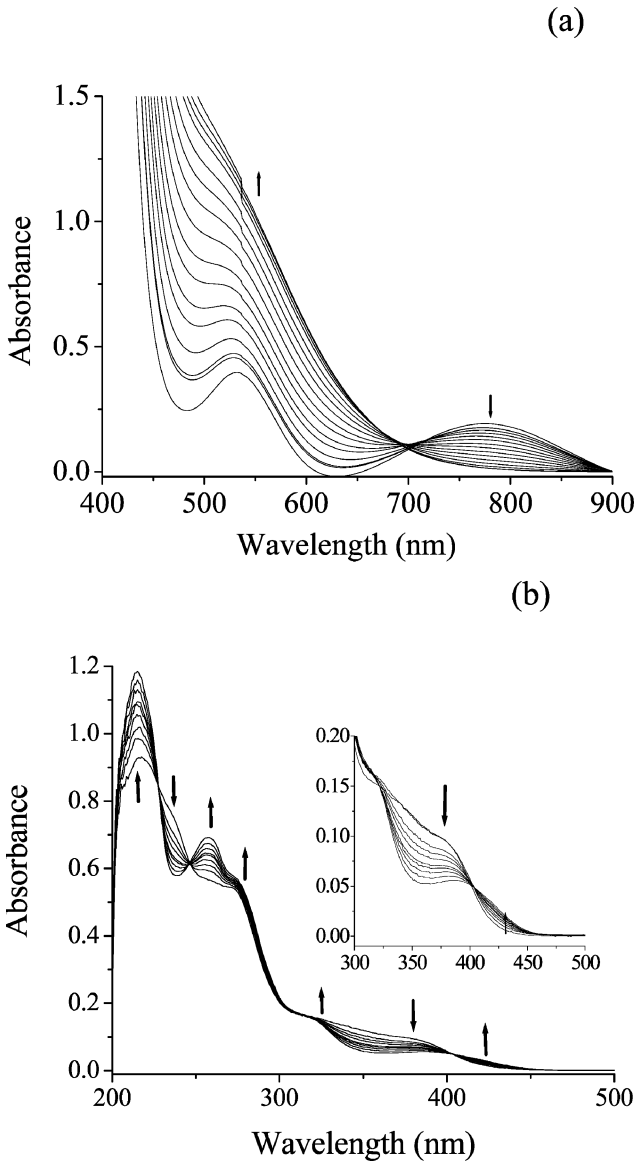

Fig. 5 UV-Vis spectral changes observed during titration of [VO(sal–his)(acac)] **3** with H_2O_2. (a) The spectra were recorded after successive additions of one drop portions of H_2O_2 (6.6×10^{-4} mmol of 30% H_2O_2 dissolved in 10 mL of methanol) to 50 mL of *ca*. 10^{-3} M solution of **3** in methanol. (b) The equivalent titration, but with lower concentrations of a [$V^{IV}O$(sal–his)(acac)] **3** solution (*ca*. 10^{-4} M); the inset shows an enlargement of the 300–500 nm region.

methanol), the band appearing at 322 nm slowly disappears with band tailing, possibly due to the formation of a diperoxo species.

Stepwise addition of 2 equiv. of H_2O_2 (0.5, 1, 1.5 and 2 equiv) to a methanolic solution of **3** leads to slight increases in $A_{\parallel}$ from 161.8 to 164 $\times 10^4$ cm^{-1}, suggesting some change in the coordination/solvation environment of **3** (Fig. 6). Simultaneously the intensity of the spectrum decreases, and after the addition of the 2 equiv of H_2O_2 the EPR intensity becomes ca. 1/5 that of the initial solution. The ^{51}V NMR of these solutions confirmed the presence of compound **4** (and also **5**, see below). Subsequent addition of 2 equiv. of methyl phenyl sulfide gave spectra with the same values of parameters g and A, the EPR signal increasing to ~50% of that of the initial solution, indicating the reversibility of the redox process occurring during the catalytic reaction.

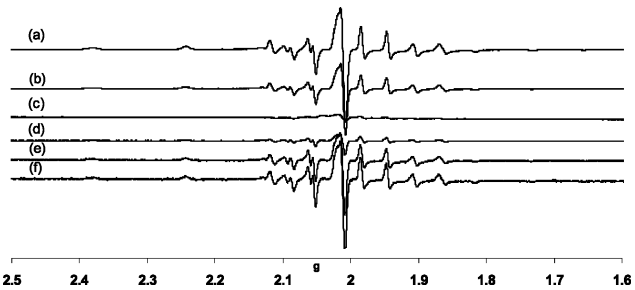

Fig. 6 Treatment of compound **3** with 30% H_2O_2 followed by the addition of methyl phenyl sulfide; (a) in MeOH; (b) 0.5 equiv. H_2O_2; (c) 2.0 equiv. H_2O_2; (d) 1.0 equiv. methyl phenyl sulfoxide; (e) 2.0 equiv. methyl phenyl sulfoxide; (f) 2.0 equiv. methyl phenyl sulfoxide (after 20 h).

The V^V system was also investigated by using ^{51}V NMR spectroscopy to detect intermediate species formed during the catalytic cycle with both **3** and **4**, choosing the oxidation of methyl phenyl sulfide as a model reaction. Complex **4** in methanolic solution (3 mM) shows one strong resonance at $\delta = -547$ ppm which we assign to $[V^VO_2(sal–his)]$ **4**. This solution displays another minor (2.3%) signal at $\delta = -558$ ppm (Fig. 7a). Both values are expected for V^VO_2 complexes having a O/N donor set.[37] We tentatively assign the −558 ppm peak to the dioxidovanadium(v) species $[V^VO_2(sal–his)(MeOH \text{ or } H_2O)]$ **5**.

Upon successive additions of 30% H_2O_2 (0.5 equiv. steps) the relative intensity of the $\delta = -547$ ppm resonance decreases, and after the addition of 1.5 equiv. of H_2O_2, a peak is detected at $\delta = -579$ ppm, which we assign to $[V^VO(O)_2(sal–his)]$ **6**. These observations are in agreement with the UV-Vis data discussed above.

This reaction mixture was divided into two portions. In the first portion, upon addition of methyl phenyl sulfide, the peroxovanadium(v) species **6** disappears immediately, with concomitant production of **4** (Fig. 7e), indicating that **6** is one of the relevant species in the reaction with the sulfide. The final ^{51}V NMR spectrum was identical to the initial spectrum of **4**, but the global intensity of the ^{51}V NMR signals decreased.

The second portion of the reaction mixture (see Fig. S4 of the ESI†) after *ca*. 20 h gave only one intense signal corresponding to **4**, indicating that formation of monoperoxovanadium(v) was reversible. Addition of 0.5 equiv. of H_2O_2 regenerated the signal corresponding to $[V^VO(O)_2(sal–his)]$ **6**, along with a new signal at $\delta = -729$ ppm. We tentatively assign this signal to the formation of

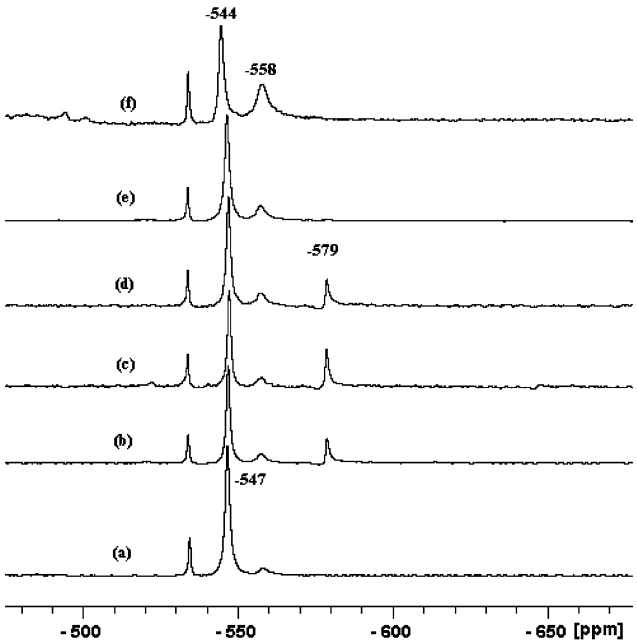

Fig. 7 ^{51}V NMR spectra for $[V^VO_2(sal–his)]$ **4**: (a) in MeOH, (b) 0.5 equiv. H_2O_2; (c) 1.5 equiv. H_2O_2; (d) 1.0 equiv. methyl phenyl sulfide; (e) 2.0 equiv. methyl phenyl sulfide; (f) after 20 h. All spectra were recorded including an external reference of aqueous vanadate at pH ~12 (peak at ca. −536 ppm).

bisperoxovanadium imidazole monoanion, $[V^VO(O_2)_2(sal–his)]^-$ **10** (see Scheme 5), with the sp^2 nitrogen atom of imidazole coordinated to the vanadium center, which is consistent with previously reported chemical shifts for similar coordination modes.[37,38,39a] Another possibility for this peak is the formation of $H_xVO_2(O_2)_2^{(3-x)-}$.[39b]

On further addition of 0.5 equiv. portions of H_2O_2 three new signals at $\delta = -715$ ppm (**11**), −668 ppm (**12**) and −648 ppm (**13**) are detected, which increase in intensity (Fig. S4 of the ESI†) and correspond to various types of peroxo complexes (tentative assignments are presented in Scheme 5).

The addition of methyl phenyl sulfide to the same reaction mixture resulted in the disappearance of the peaks of **6**, **10**, **11**, **12** and **13** (Fig. S4 and Scheme 5). The fact that a ^{51}V NMR spectrum similar to the initial one (the solution of **4** in MeOH) is now obtained, confirms the reversibility of the processes involving complex **4**, namely the regeneration of **4** after the addition of H_2O_2, formation of an oxidoperoxo complex and its reaction with the sulfide.

Solutions of **4** in methanol are also sensitive to pH changes, which were also monitored by ^{51}V NMR spectroscopy. Addition of 1 equiv. of HCl to a methanolic solution of **4** resulted in a reduction in intensity of the $\delta = -547$ ppm and $\delta = -558$ ppm peaks, while a new signal at $\delta = -524$ ppm was detected (Fig. S5 of the ESI†). Further addition of 1 equiv. of HCl gave a spectrum with only one intense signal at $\delta = -524$ ppm. We assign this to the protonation of the imidazole N atom, the sal–his ligand becoming bidentate and the solvent also coordinating $[V^VO_2(sal-Hhis)(MeOH)]$ ($\delta = -524$ ppm) **7** (see Scheme 5). A rather similar explanation was given by Pecoraro and coworkers[21] for the $V^{IV}O$ with the same ligand system.

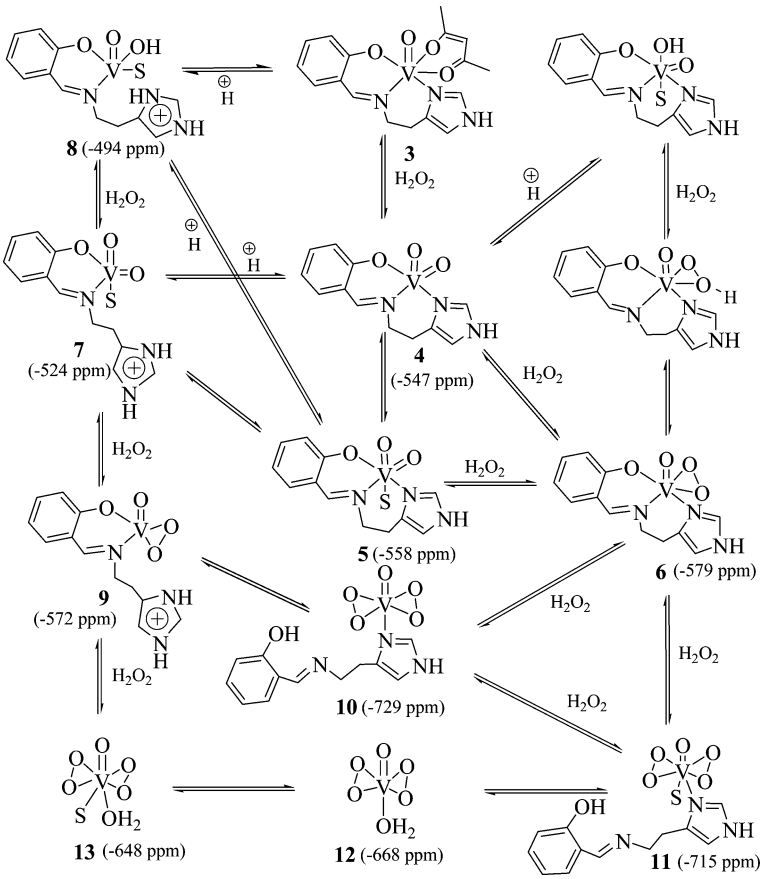

Scheme 5 Proposed reaction scheme (see text) and tentative assignments of the ^{51}V NMR chemical shifts involving oxidovanadium(v)-, dioxidovanadium(v)-, monoperoxovanadium(v)- and bisperoxovanadium(v)-species formed in methanolic solutions of **3** and **4** based on ^{51}V NMR spectroscopy, on addition of aqueous H_2O_2, HCl and methyl phenyl sulfide (this may cause reduction to **3**). S indicates solvent.

As compound **3** is paramagnetic, no signal was observed by ^{51}V NMR spectroscopy when dissolved in methanol. However, after addition of 0.5 equiv. of H_2O_2, three signals ($\delta = -494$, -547 and -558 ppm) appear (Fig. 8), and we tentatively assign them to $[V^{V}O(OH)(sal\text{-}Hhis)(MeOH)]$ ($\delta = -494$ ppm) **8**, $[V^{V}O_2(sal\text{–}his)]$ ($\delta = -547$ ppm) **4** and $\{[V^{V}O_2(sal\text{–}his)(MeOH)]$ ($\delta = -558$ ppm) **5** (Fig. 8). Upon further addition of 0.5 equiv. of H_2O_2 another three signals at: $\delta = -579$, -524 and -572 ppm were detected, which we tentatively assign as $[V^{V}O(O_2)(sal\text{–}his)]$ ($\delta = -579$ ppm) **6**, $\{[V^{V}O_2(sal\text{-}Hhis)(MeOH)]$ ($\delta = -524$ ppm) **7** and $[V^{V}O(O_2)(sal\text{-}Hhis)]^{+}$ ($\delta = -572$ ppm) **9**. Further addition of 0.5 equiv. portions of H_2O_2 resulted in the formation of the peak at -729 ppm (see above), and $[VO(O_2)_2(H_2O)(MeOH)]^{-}$ ($\delta = -648$ ppm), **13**.

Upon addition of methyl phenyl sulfide (spectra h–j in Fig. 8), the monoperoxovanadium(v) and bisperoxovanadium(v) species are consumed, and the final ^{51}V NMR spectrum showed only two major signals identical to the initial spectrum of methanolic solutions of **4**, showing that the V^{V} catalyst is regenerated after the consumption of H_2O_2. Besides having an easily measurable ^{51}V NMR spectrum, for this solution a reasonably intense EPR spectrum was also recorded. This confirmed the formation of **3**, and even after 5 d a similar EPR spectra could be obtained.

In Scheme 5 we summarize our observations regarding the reaction processes involving **3** and **4** in MeOH solutions, as measured by ^{51}V NMR and EPR spectroscopy.

Mechanism of sulfide oxidation

It is well known that V^{V}-peroxo compounds mediate oxygenation reactions including the oxidation of sulfides to sulfoxides and sulfones and the epoxidation of alkenes and allylic alcohols.[40]

The sulfur atom of methyl phenyl sulfide is electron-rich and undergoes electrophilic oxidation giving the sulfoxide. We clearly demonstrated that complexes **3** and **4** are able to generate monoperoxo and even bisperoxovanadium(v) species on treatment with H_2O_2. The peroxo complexes being stable and detectable, it is likely that hydroperoxovanadium(v) complexes also form as aqueous H_2O_2 is being added and the pH decreases, enhancing the electrophilicity of the coordinated peroxo ligand and facilitating the nucleophilic attack by the sulfide. An outline of the catalytic cycle for oxidation of methyl phenyl sulfide, which has also been proposed by other authors[21,27,41] is given in Scheme 6.

Conclusions

The compound Hsal–his **I** derived from salicylaldehyde and histamine has been covalently bonded to chloromethylated polystyrene cross-linked with 5% divinylbenzene. Upon reaction with $[V^{IV}O(acac)_2]$ the complex PS–$[V^{IV}O(sal\text{–}his)(acac)]$ **1** was obtained, which, upon oxidation, yielded the dioxidovanadium(v) PS–$[V^{V}O_2(sal\text{–}his)]$ **2**. The corresponding non polymer-bound

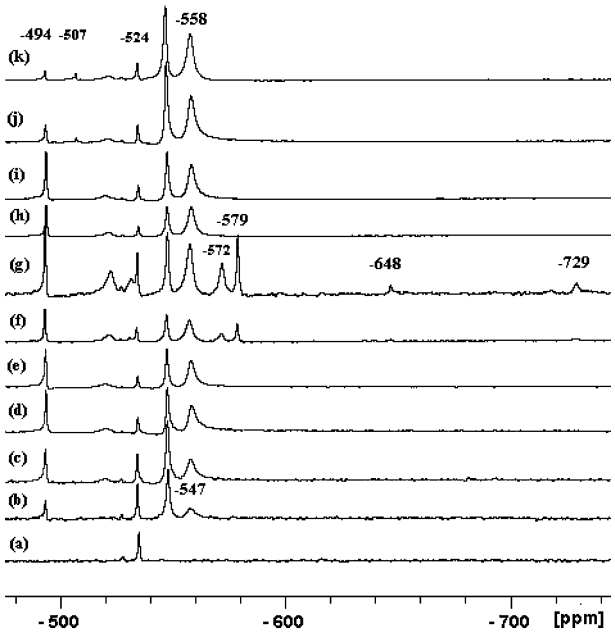

Fig. 8 ^{51}V NMR spectra for [V^{IV}O(sal–his)(acac)] **3**: (a) in MeOH, (b) 0.5 equiv. H_2O_2; (c) 1.0 equiv. H_2O_2; (d,e) 1.5 equiv. H_2O_2; (f) 2.0 equiv. H_2O_2; (g) 2.5 equiv. H_2O_2; (h) 1.0 equiv. methyl phenyl sulfide; (i) 2.0 equiv. methyl phenyl sulfide; (j) 3.0 equiv. methyl phenyl sulfide (k) 3.0 equiv. methyl phenyl sulfide (after 24 h). All spectra were recorded including an external reference of aqueous vanadate at pH ~12 (peak at ca. −536 ppm).

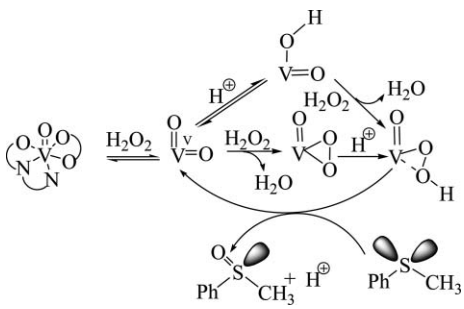

Scheme 6 Reaction mechanism of oxidation of methyl phenyl sulfide as a model substrate for sulfoxidations.

complexes [V^{IV}O(sal–his)(acac)] **3** and [$V^{V}O_2$(sal–his)] **4** have also been prepared and characterised. Complexes **1** and **2** have been used as catalysts for the oxidation of methyl phenyl sulfide, diphenyl sulfide and benzoin with aqueous H_2O_2 as an oxidant. Under the optimised reaction conditions, a maximum of *ca*. 94% conversion of methyl phenyl sulfide, and *ca*. 83% of diphenyl sulfide has been achieved in 2 h, with significant amounts of the corresponding sulfones. A maximum of 91.2% conversion of benzoin has been achieved within 6 h. The corresponding neat complexes gave slightly lower conversions and selectivity, but significantly lower turnover frequencies. Moreover, the polymer-bound catalysts did not leach during catalytic action and are recyclable, further emphasizing their advantage over the neat complexes.

UV-Vis, EPR and ^{51}V NMR spectroscopy were used to characterize methanolic solutions of **3** and **4** and to identify species formed upon addition of H_2O_2 and/or acid, similar oxido, peroxo or peroxo species being detected by ^{51}V NMR spectroscopy starting either with solutions of **3** or of **4**. Addition of methyl phenyl sulfide to solutions containing peroxo species promoted the oxidation of the sulfide and regenerated the formation of the V^{IV} species formed upon dissolution of **4** or oxidation of **3**. The EPR spectra also confirm that [V^{IV}O(sal–his)(acac)] **3** is also present in these solutions if the starting product is complex **3**. These studies confirm that most of these reactions involving complexes **3** or **4** are reversible, therefore supporting the catalytic nature of the sulfide oxidation processes.

Acknowledgements

Department of Science and Technology, Government of India, New Delhi is gratefully acknowledged for financial support of the work. A.A. thanks IITR for the MHRD fellowship. The authors also wish to thank FEDER, Fundação para a Ciência e a Tecnologia, POCI 2010 (namely PPCDT/QUI/55985/2004, PPCDT/QUI/56946/2004, and SFRH/BPD/34835/2007 programs).

References

1 M. Weyand, H. J. Hecht, M. Kiess, M. F. Liaud, H. Vilter and D. Schomburg, *J. Mol. Biol.*, 1999, **293**, 595–611.
2 J. N. Carter-Franklin, J. D. Parrish, R. A. Tchirret-Guth, R. D. Little and A. Butler, *J. Am. Chem. Soc.*, 2003, **125**, 3688–3689.
3 D. Rehder, G. Santoni, G. M. Licini, C. Schulzke and B. Meier, *Coord. Chem. Rev.*, 2003, **237**, 53–63.
4 A. Butler, *Coord. Chem. Rev.*, 1999, **187**, 17–35.
5 G. J. Colpas, B. J. Hamstra, J. W. Kampf and V. L. Pecoraro, *J. Am. Chem. Soc.*, 1996, **118**, 3469–3478.
6 B. J. Hamstra, G. J. Colpas and V. L. Pecoraro, *Inorg. Chem.*, 1998, **37**, 949–955.
7 D. Rehder, *Bioinorganic Vanadium Chemistry*, John Wiley & Sons, New York, 2008.
8 P. P. Knops-Gerrits, D. D. Vos, F. Thibault-Starzyk and P. A. Jacobs, *Nature*, 1994, **369**, 543–546.
9 G. S. Mishra and A. Kumar, *Catal. Lett.*, 2002, **81**, 113–117.
10 T. Joseph, D. Srinivas, C. S. Gopinath and S. B. Halligudi, *Catal. Lett.*, 2002, **83**, 209–214.
11 P. A. Awasarkar, S. Gopinathan and C. Gopinathan, *Synth. React. Inorg. Met.–Org. Chem.*, 1985, **15**, 133–147.
12 R. H. Groeneman, L. R. MacGillivray and J. L. Atwood, *Inorg. Chem.*, 1999, **38**, 208–209.
13 D. A. Annis and E. N. Jacobson, *J. Am. Chem. Soc.*, 1999, **121**, 4147–4154.
14 J. K. Karjalainen, O. E. O. Harmi and D. C. Sherrington, *Molecules*, 1999, **3**, 51–59.
15 L. Canali and D. C. Sherrington, *Chem. Soc. Rev.*, 1999, **28**, 85–93.
16 D. C. Sherrington, *Catal. Today*, 2000, **57**, 87–104.
17 M. R. Maurya, U. Kumar and P. Manikandan, *Eur. J. Inorg. Chem.*, 2007, 2303–2314.
18 M. R. Maurya, U. Kumar, I. Correia, P. Adão and J. Costa Pessoa, *Eur. J. Inorg. Chem.*, 2008, 577–587.
19 M. R. Maurya, M. Kumar, A. Kumar and J. Costa Pessoa, *Dalton Trans.*, 2008, 4220–4232.
20 R. A. Rowe and M. M. Jones, *Inorg. Synth.*, 1957, **5**, 113–116.
21 C. R. Cornman, J. Kampf, M. S. Lah and V. L. Pecoraro, *Inorg. Chem.*, 1992, **31**, 2035–2043.
22 A. Rockenbauer and L. Korecz, *Appl. Magn. Reson.*, 1996, **10**, 29–43.
23 M. M. Miller and D. C. Sherrington, *J. Catal.*, 1995, **152**, 368–376.
24 M. R. Maurya, *Coord. Chem. Rev.*, 2003, **237**, 163–181.
25 K. Wuethrich, *Helv. Chim. Acta*, 1965, **48**, 1012–1017.
26 (*a*) N. D. Chasteen, in: *Biological Magnetic Resonance*, ed. J. Reuben, Plenum, New York, 1981, 53; (*b*) E. Garribba, G. Micera, and D. Sanna, *6th International Vanadium Symposium, Lisbon, 2008, book of abstracts*, O30.

27 T. S. Smith II, C. A. Root, J. W. Kampf, P. G. Rasmussen and V. L. Pecoraro, *J. Am. Chem. Soc.*, 2000, **122**, 767–775.

28 (*a*) K. Nakajima, M. Kojima and J. Fujita, *Chem. Lett.*, 1986, **9**, 1483–1486; (*b*) C. Bolm and F. Bienewald, *Angew. Chem., Int. Ed. Engl.*, 1995, **34**, 2883–2885; (*c*) K. Nakajima, K. Kojima, M. Kojima and J. Fujita, *Bull. Chem. Soc. Jpn.*, 1990, **63**, 2620–2630; (*d*) J. Skarzewski, E. Ostrycharz and R. Siedlecka, *Tetrahedron: Asymmetry*, 1999, **10**, 3457–3461; (*e*) A. H. Vetter and A. Berkessel, *Tetrahedron Lett.*, 1998, **39**, 1741–1744; (*f*) B. Pelotier, M. S. Anson, I. B. Campbell, S. J. F. Macdonald, G. Priem and R. F. W. Jackson, *Synlett*, 2002, **7**, 1055–1060.

29 (*a*) M. Palucki, P. Hanson and E. N. Jacobsen, *Tetrahedron Lett.*, 1992, **33**, 7111–7114; (*b*) K. Noda, N. Hosoya, R. Irie, Y. Yamashita and T. Katsuki, *Tetrahedron*, 1994, **50**, 9609–9618.

30 (*a*) S. Colonna, A. Manfredi, M. Spadoni, L. Casella and M. Gulloti, *J. Chem. Soc., Perkin Trans. 1*, 1981, 71; (*b*) C. Sasaki, K. Nakajima, M. Kojima and J. Fujita, *Bull. Chem. Soc. Jpn.*, 1991, **64**, 1318–1324.

31 R. A. Sheldon and J. K. Kochi, *Metal Catalyzed Oxidations of Organic Compounds*, Academic Press, New York, 1981.

32 S. V. Ley and A. Madin in *Comprehensive Organic Synthesis*, ed. B. M. Trost, I. Fleming and S. V. Ley, vol. 7, Pergamon, Oxford, 1991, p. 251.

33 I. Flament and M. Stoll, *Helv. Chim. Acta*, 1967, **50**, 1754–1758.

34 H. Wynberg and H. J. Kooreman, *J. Am. Chem. Soc.*, 1965, **87**, 1739–1742.

35 W. W. Paudler and J. M. Barton, *J. Org. Chem.*, 1966, **31**, 1720–1722.

36 G. B. Gill, in *Comprehensive Organic Synthesis*, ed. G. Pattenden, vol. 3, Pergamon Press, New York, 1991, p. 821–838.

37 D. Rehder, C. Weidemann, A. Duch and W. Priebsch, *Inorg. Chem.*, 1988, **27**, 584–587.

38 (*a*) V. Conte, F. D. Furia and S. Moro, *J. Mol. Catal.*, 1995, **104**, 159–169; (*b*) D. C. Crans, A. D. Keramidas, H. Hoover-Litty, O. P. Anderson, M. M. Miller, L. M. Lemoine, S. Pleastic-Williams, M. Vandenberg, A. J. Rossomando and L. J. Sweet, *J. Am. Chem. Soc.*, 1997, **119**, 5447–5448; (*c*) J. S. Jaswal and A. S. Tracey, *J. Am. Chem. Soc.*, 1993, **115**, 5600–5607; (*d*) K. P. Bryliakov, N. N. Karpyshev, S. A. Fominsky, A. G. Tolstikov and E. P. Talsi, *J. Mol. Catal.*, 2001, **171**, 73–80.

39 (*a*) V. Conte, F. D. Furia and S. Moro, *J. Mol. Catal.*, 1994, **94**, 323–333; (*b*) J. S. Jaswal and A. S. Tracey, *Inorg. Chem.*, 1991, **30**, 3718–3722.

40 (*a*) A. Butler, M. J. Clague and G. E. Maister, *Chem. Rev.*, 1994, **94**, 625–638; (*b*) O. Bortolini, F. Di Furia and G. Modena, *J. Mol. Catal.*, 1982, **16**, 61–68; (*c*) M. J. Clague, N. L. Keder and A. Butler, *Inorg. Chem.*, 1993, **32**, 4754–4761; (*d*) A. Butler and M. J. Clague in *Mechanistic Bioinorganic Chemistry, Adv. Chem. Ser.*, ed. H. H. Thorp and V. L. Pecoraro, 1995, **246**, 329; (*e*) A. Butler and A. H. Baldwin in *Structure and Bonding*, ed. P. Sadler, H. A. O. Hill and A. Thompson, Springer Verlag, Berlin, 1997, 109; (*f*) V. Conte, F. Di Furia and S. Moro, *J. Phys. Org. Chem.*, 1996, **9**, 329–336; (*g*) O. Bortolini, M. Carraro, V. Conte and S. Moro, *Eur. J. Inorg. Chem.*, 1999, 1489–1495; (*h*) G. Santoni, G. Licini and D. Rehder, *Chem.–Eur. J.*, 2003, 4700–4708.

41 (*a*) C. J. Schneider, J. E. Penner-Hahn and V. L. Pecoraro, *J. Am. Chem. Soc.*, 2008, **130**, 2712–2713; (*b*) C. R. Cornman, G. J. Colpas, J. D. Hoeschele, J. Kampf and V. L. Pecoraro, *J. Am. Chem. Soc.*, 1992, **114**, 9925–9953; (*c*) C. R. Cornman, J. Kampf and V. L. Pecoraro, *Inorg. Chem.*, 1992, **31**, 1983–1985; (*d*) G. Zampella, P. Fantucci, V. L. Pecoraro and L. De Gioia, *J. Am. Chem. Soc.*, 2005, **127**, 953–960; (*e*) T. S. Smith, II and V. L. Pecoraro, *Inorg. Chem.*, 2002, **41**, 6754–6760; (*f*) R. I. de la Rosa, M. J. Clague and A. Butler;, *J. Am. Chem. Soc.*, 1992, **114**, 760–761.